

**THE DARK CONNECTION BETWEEN THE EGRET EXCESS OF
DIFFUSE GALACTIC GAMMA RAYS, THE CANIS MAJOR DWARF,
THE MONOCEROS RING, THE INTEGRAL 511 keV ANNIHILATION
LINE, THE GAS FLARING AND THE GALACTIC ROTATION CURVE.**

W. DE BOER

*University of Karlsruhe
Postfach 6980, D-76131 Karlsruhe, Germany
E-mail: wim.de.boer@cern.ch

The EGRET excess of diffuse Galactic gamma rays shows all the key features of dark matter annihilation (DMA) for a WIMP mass in the range 50-100 GeV, especially the distribution of the excess is compatible with a standard halo profile with some additional ringlike substructures at 4 and 13 kpc from the Galactic centre. These substructures coincide with the gravitational potential well expected from the ring of dust at 4 kpc and the tidal stream of dark matter from the Canis Major satellite galaxy at 13 kpc, as deduced from N-body simulations fitting to the Monoceros ring of stars. Strong independent support for this substructure is given by the gas flaring in our Galaxy. The gamma rays from DMA are originating predominantly from the hadronization of mono-energetic quarks, which should produce also a small, but known fraction of protons and antiprotons. Bergström et al. an antiproton flux far above the observed antiproton flux and they conclude that the DMA interpretation of the EGRET excess can therefore be excluded. However, they used an isotropic propagation model, i.e. the same diffusive propagation in the disk and the halo. It is shown that an anisotropic propagation model is consistent with the EGRET gamma ray excess, the antiproton flux and the ratios of secondary/primary and unstable/stable cosmic ray particles. Such an anisotropic propagation is supported by the large bulge/disk ratio of the positron annihilation line, as observed by the INTEGRAL satellite. In this case no need for new sources specific to the bulge are needed, so the claimed evidence for strong DMA in the bulge from these observations is strongly propagation model dependent. In the framework of Supersymmetry cross section predictions for direct dark matter searches are presented taking into account the EGRET data, the WMAP data and other electroweak constraints.

1. Introduction

Cold Dark Matter (CDM) is well established by the high rotation speeds in galaxies and clusters of galaxies. Recent cosmological measurements yield a dark matter (DM) density of $22 \pm 2\%$ of the energy of the Universe.¹ If this DM is created thermally during the Big Bang the present relic density is inversely proportional to $\langle\sigma v\rangle$, the annihilation cross section σ of DM particles, usually called WIMPS

(Weakly Interacting Massive Particles), times their relative velocity. The average is taken over these velocities. This inverse proportionality is obvious, if one considers that a higher annihilation rate, given by $\langle\sigma v\rangle n_\chi$, would have reduced the relic density before freeze-out, i.e. the time, when the expansion rate of the Universe, given by the Hubble constant, became equal to or larger than the annihilation rate. The relation can be written as:²

$$\Omega_\chi h^2 = \frac{m_\chi n_\chi}{\rho_c} h^2 \approx \left(\frac{3 \cdot 10^{-27} \text{cm}^3 \text{s}^{-1}}{\langle\sigma v\rangle} \right). \quad (1)$$

For the present value of $\Omega h^2 = 0.105 \pm 0.008$, as measured by WMAP,¹ the thermally averaged total cross section at the freeze-out temperature of $m_\chi/22$ must have been around $3 \cdot 10^{-26} \text{cm}^3 \text{s}^{-1}$. Note that $\langle\sigma v\rangle$ as calculated from Eq. 1 is independent of the WIMP mass (except for logarithmic corrections) as can be shown by detailed calculations.³ If the s-wave annihilation is dominant, as expected in many supersymmetric models, then the annihilation cross section is energy independent, i.e. the cross section given above is also valid for the cold temperatures of the present universe.⁴ Such a large cross section will lead to a production rate of mono-energetic quarks^a in our Galaxy, which is 40 orders of magnitude above the rate produced at any accelerator. The fragmentation of these mono-energetic quarks will lead to a large flux of neutrinos, photons, protons, antiprotons, electrons and positrons in the Galaxy. From these, the protons and electrons disappear in the sea of many matter particles, but the photons and antimatter particles may be detectable above the background, generated by cosmic ray interactions with the gas in the Galaxy. Such searches for indirect Dark Matter detection have been actively pursued. Recent reviews and references to earlier work can be found in Refs.⁵⁻⁷

Gamma rays have the advantage that they point back to the source and do not suffer energy losses, so they are the ideal candidates to trace the dark matter density and have a spectral shape characteristic for mono-energetic quarks. The charged components interact with Galactic matter and are deflected by the Galactic magnetic field, so they do not point back to the source. Therefore the charged particle fluxes have large uncertainties from the propagation models, which determine how many of the produced particles arrive at the detector. For gamma rays the propagation is straightforward: only the ones pointing towards the detector will be observed.

An excess of diffuse gamma rays compatible with dark matter annihilation

^aThe quarks are mono-energetic, since the kinetic energy of the cold dark matter particles is expected to be negligible with the mass of the particles, so the energy of the quarks equals the mass of the WIMP.

(DMA) has indeed been observed by the EGRET telescope on board of NASA's CGRO (Compton Gamma Ray Observatory).⁸ Below 1 GeV the CR interactions describe the data perfectly well, but above 1 GeV the data are up to a factor two above the expected background. The excess shows all the features of DMA annihilation for a WIMP mass between 50 and 70 GeV.⁹ Masses up to 100 GeV are possible if one assumes the cosmic ray energy spectrum to vary in the Galaxy. The excess was observed in all sky directions, which would imply that DM is not dark anymore, but shining in gamma rays.⁹ Of course, such an important observation needs to be scrutinized heavily. Among the most important criticism was a paper by Bergström et al.¹⁰ claiming that the antiproton flux from DMA, using the DM distribution from the EGRET excess, would be an order of magnitude higher than the observed antiproton flux. However, they use an isotropic propagation model with the *same* propagation in the disk and the halo. For the expected anisotropic propagation models everything can be made consistent by having a faster propagation perpendicular to the disk than in the disk, in which case the antiprotons from DMA in the halo do not return to the disk. This demonstrates the large uncertainties from propagation models for indirect dark matter searches.

It is interesting to note that anisotropic propagation models can easily explain a large bulge/disk (B/D) ratio of the positron annihilation, as observed from the intensity of the 511 keV annihilation line of thermalized positrons. These positrons are e.g. produced in the β -decays of radioactive nuclei from supernova explosions. A large B/D ratio is simply due to the different geometries of the disk and the bulge: in the bulge the positrons and electrons can annihilate and radiate before escaping to the halo, in the disk they enter the halo much faster without having time to radiate and/or annihilate. In contrast, in isotropic propagation models one can only explain the large bulge/disk ratio by a new source for positrons for the bulge alone. Anisotropic propagation models have enough freedom to explain the results without new sources. So the claimed evidence for DMA from these observations¹³ are strongly propagation model dependent.

The paper is organized as follows: in section 2 we summarize the DMA interpretation of the EGRET excess. In section 3 we discuss the problems with the isotropic propagation models. An anisotropic propagation model, which simultaneously describes the antiproton flux, the EGRET excess and the observations concerning primary and secondary cosmic rays and cosmic clocks is discussed in section 4, while in section 5 the consequences for the INTEGRAL excess of the 511 keV line in this anisotropic propagation model are discussed. In section 6 the constraints from direct dark matter searches are discussed. Section 7 summarizes the results.

2. The DMA Interpretation of the EGRET Excess of diffuse Galactic Gamma Rays

It is well known that the EGRET satellite data on diffuse gamma rays shows an excess above 1 GeV in comparison with the expectations from CR interactions.⁸ Below 1 GeV the CR interactions describe the data perfectly well. The excess shows all the features of DMA annihilation for a WIMP mass between 50 and 70 GeV.⁹ Especially, the two basic constraints expected from any indirect DMA signal are fulfilled:

- the excess should have the same spectral shape in all sky directions.
- the excess should be observable in a large fraction of the sky with an intensity distribution corresponding to the gravitational potential of our Galaxy. The latter means that one should be able to relate the distribution of the excess to the rotation curve.

The analysis of the EGRET data is simplified by the fact that the spectral shapes of the DMA contribution and the background from CR interactions with the gas of the disk are well known from accelerator experiments: (i) the DMA signal should have the gamma ray spectrum from the fragmentation of mono-energetic quarks, which has been studied in great detail at LEP.¹⁴ (ii) the background in the energy range of interest is dominated by CR protons hitting the hydrogen of the disk. Therefore the dominant background spectral shape is known from fixed-target experiments. Given that these shapes are known from the two best studied reactions in accelerator experiments allows to fit these *known* shapes to the observed gamma ray spectrum in a given sky direction and obtain from the fitted normalization constants the contribution of both background and annihilation signal. So in this case one does not need propagation models to estimate the background, since the data itself calibrates the amount of background. A typical spectrum is shown in Fig. 1, which clearly shows the rather distinct shapes of DMA and background, so the two normalization constants are not strongly correlated. The shape of the DMA contribution shifts to the right for heavier WIMP masses. The preferred WIMP mass is between 50 and 70 GeV with a maximum allowed value of 100 GeV.⁹ Repeating these fits over 180 independent sky directions showed that indeed: (i) the *shape* of EGRET excess is consistent with a 60 GeV WIMP mass in each sky direction (ii) the *intensities* of the EGRET excess in various sky directions are as expected from the gravitational potential, which could be proven by reconstructing the rotation curve from the EGRET data after adding the known distribution of visible matter to the DM halo.⁹ A parametrization of the best fitted DM halo is shown in Fig. 1 on the right hand side, which clearly shows the ringlike structures at 4 and 13 kpc, as determined from the enhanced intensity of the EGRET excess

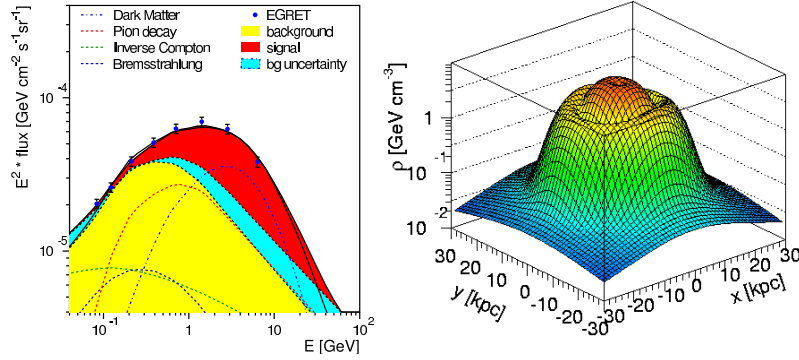


Fig. 1: Left: Fit of the shapes of background and DMA signal to the EGRET data in the direction of the Galactic centre. The dark shaded (red) area indicates the signal contribution from DMA for a 60 GeV WIMP mass using the shape from high energy electron-positron annihilation experiments, while the area below it represents the background with the various indicated contributions. The (blue) area between the dotted lines just below the shaded area is the estimated uncertainty in the background, which is dominated by solar modulation. The normalization of both the background and the DMA contribution have been left free in the fit of the known shapes. Right: Parametrization of the dark matter density profile as determined from the distribution of the EGRET excess in the sky. Both pictures are taken from Ref.⁹

in these regions. The ring at 4 kpc (inner ring) coincides with the ring of dust in this region. The dust is presumably kept there because of a gravitational potential well, which is provided by the ring of DM. The ring at 13 kpc (outer ring) is thought to originate from the tidal disruption of the Canis Major dwarf galaxy, which circles the Galaxy in an almost circular orbit coplanar with the disk.^{15–19} Three independent observations confirm this picture of the ring originating from the tidal disruption of a dwarf galaxy:

(i) a ring of DM is expected in this region from the observed ring of stars, called Monoceros ring, which was discovered first with SDSS data.^{20,21} Follow-up observations²² found that this structure surrounds the Galactic disk as a giant ring (observed over 100 degrees in latitude) at Galactocentric distances from 8 kpc to 20 kpc. Tracing this structure with 2MASS M giant stars,²³ suggested that this structure might be the result from the tidal disruption of a merging dwarf galaxy. N-body simulations show indeed that the overdensity in Canis Major is indeed a

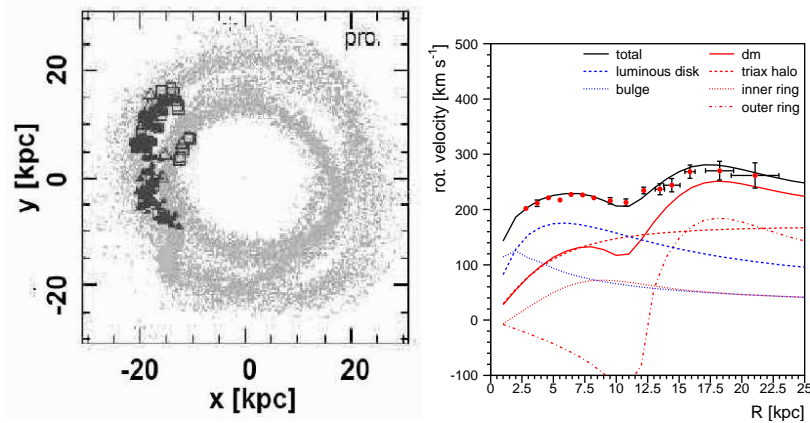


Fig. 2: Left: results of an N-body simulation of the tidal disruption of the Canis Major dwarf Galaxy, whose orbit was fitted to the observed stars (symbols). The simulation predicts a ringlike structure of dark matter with a radius of 13 kpc. From Ref.¹⁶ Right: The rotation curve with the contributions of the bulge, the disk, the triaxial dark matter halo and the two ringlike structures. The outer ring causes the peculiar change of slope in the rotation curve at about 11 kpc. From Ref.⁹

perfect progenitor for the Monoceros stream and they predict a DM ring at 13 kpc with a low ellipticity and almost coplanar with the disk, as shown in the left panel of Fig. 2. The orientation of the major axis at an angle of 20 degrees with respect to the axis sun-Galactic centre and the ratio of minor to major axis around 0.8 agrees with the EGRET ring parameters given in Ref.⁹ This correlation with the EGRET excess lends both support to the DMA interpretation of the EGRET excess *and* the interpretation that the Monoceros stream originates from the tidal disruption of the Canis Major (CM) satellite galaxy, thus rejecting the interpretation that the overdensity of stars forming the Canis Major dwarf is a warp of the Galactic disk (see discussions e.g. in Refs.^{24,25}). A further rejection from the hypothesis that the CM overdensity is just due to the warp comes from the gas flaring discussed below, which shows that the Monoceros stream is connected to an enormous amount of dark matter.

(ii) Such a massive ring structure influences the rotation curve in a peculiar way: it decreases the rotation curve at radii inside the ring and increases it outside. This is apparent from the change in direction of the gravitational force from the ring on a tracer, since this force decreases the force from the galactic centre for

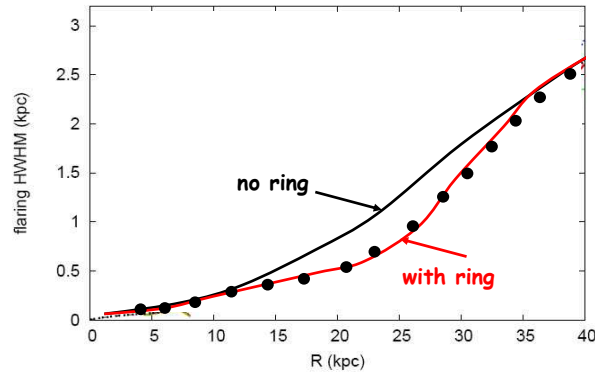


Fig. 3: The half-width-half-maximum (HWHM) of the gas layer of the Galactic disk as function of the distance from the Galactic center. Clearly, the fit including a ring of dark matter above 10 kpc describes the data much better. Adapted from data in Ref.²⁶

a tracer inside the ring, but increases it outside the ring. This is indeed observed as shown in the right hand panel of Fig. 2, where the negative contribution of the outer ring is clearly visible.

(iii) A direct proof of the large amount of DM mass in the outer ring comes from a recent analysis of the gas flaring in our Galaxy.²⁶ Using the new data of the LAB survey of the 21 cm line in our Galaxy led to a precise measurement of the gas layer thickness up to radii of 40 kpc. The increase of the half width of the layer after a decrease to half its maximum value (HWHM) as function of distance is governed by the decrease in gravitational potential of the disk. The outer ring increases the gravitational potential above 10 kpc, which is expected to reduce the gas flaring. Only after taking the ring like structure into account the reduced gas flaring in this region could be understood. The effect is shown in Fig. 3. A fit averaged over all longitudes requires a DM ring with a mass of 2.10^{10} solar masses, in rough agreement with the EGRET excess.

Clearly, these three independent astronomical observations need a ringlike DM structure above 10 kpc, thus providing independent evidence for the DMA interpretation of the EGRET excess.

These independent observations *cannot* be explained by alternative explanations of the EGRET excess, of which the strongest one is provided by the "op-

timized” model.²⁷ In this case the cosmic ray spectrum of protons and electrons is not taken to be the locally observed one, but modified to increase the gamma ray spectrum at high energies. This requires a strong break in the injection spectrum of electrons and protons in order not to change the gamma ray spectrum below 1 GeV, but only above 1 GeV. However, the gamma ray spectra at intermediate and high latitudes are created by the *local* cosmic rays. Still they show the excess. Furthermore, spectral shape differences are not expected, since diffusion is fast compared with the energy loss time, so diffusion equalizes the spectrum everywhere in agreement with the observation that the gamma ray spectra in all directions can be described with the *same* CR spectrum in all directions, i.e. the same spectral shape everywhere in the Galaxy.

Another explanation is provided by tuning the efficiency of the EGRET spectrometer to simulate DMA.²⁸ However, this requires the efficiency already to be modified around 1 GeV and reaching a change in efficiency of 80% at 10 GeV in clear disagreement with the calibration error in a photon beam before launch²⁹ and the residual uncertainties below 20% during the flight after correcting for time dependent effects.³⁰ Although there is some uncertainty in the efficiency of the veto counter at higher energies because of the backscatter from the calorimeter, this effect should not start at 1 GeV. Even the authors agree that the considered effects are too small individually and it is not clear that if one adds the errors all linearly that one gets effects up to 80%. And if these effects add up, it would be a remarkable coincidence that the excess corresponds exactly to the very specific sharply falling spectrum from the fragmentation of mono-energetic quarks! An even more remarkable coincidence is that the distribution of the excess in the sky follows the gravitational potential, as proven by the gas flaring and the rotation curve. Therefore the excess is not as isotropic as suggested by these authors, if one observes in finer sky bins, which reveals ringlike structures.

3. The Antiproton Flux from DMA in an Isotropic Propagation Model

As mentioned in the introduction, a serious objection about the DMA interpretation concerns the antiproton flux. However, this depends strongly on the propagation model. Here we summarize the concepts used for the “conventional” propagation model, discuss its priors and its alternatives.

The main features of our Galaxy are a barred central bulge with a diameter of a few kpc and a large spiral disk of about 15 kpc. Most of the gas is distributed in the disk, which extends to radii of 15-20 kpc, while the supernovae remnants (SNR) peak at a distance of a few kpc from the centre. They are thought to be the source of the cosmic rays (CRs) with energies up to 10^{15} eV. These CRs form a plasma of ionized particles, in which the electric fields can be neglected by virtue

of the high conductivity and the magnetic fields form Alfvén waves, i.e. a traveling oscillation of ions and the magnetic field. The ion mass density provides the inertia and the magnetic field line tension provides the restoring force. The wave propagates in the direction of the magnetic field with the Alfvén speed, although waves exist at oblique incidence and smoothly change into magnetosonic waves when the propagation is perpendicular to the magnetic field. If the wavelength of the Alfvén waves equals a multiple of the gyration radius of a CR, resonant scattering occurs, which leads to a change in pitch angle of the CR (pitch angle scattering) without changing its energy.³¹ Such a process leads to a random walk of CRs, which can be described by a diffusion equation (see review in Ref.³²). If the B-field has no preferred direction, i.e. if the turbulent small scale component is much stronger than the regular large scale component, the waves propagate randomly in all directions and the diffusion of CRs is isotropic. From the isotropy of CRs one usually assumes the propagation to be isotropic.

Most primary nuclei show a power law spectrum falling with energy like $E^{-2.7}$. This can be easily tuned by selecting the injection spectrum of the primary particles accordingly. However, since the inelastic cross sections for secondary particle production are usually not strongly energy dependent at higher energies, this would lead to rather flat spectra for the secondary/primary ratios in contrast to the observed B/C ratio, which shows a maximum at about 1 GeV/nucleon and decreases as $E^{-0.6}$ towards higher energy. This can be accommodated by assuming energetic particles diffuse faster out of the Galaxy, i.e. the diffusion constant is proportional to $E^{0.6}$. This reduces the high energy part of the B/C spectra. The decrease at low energies can be accommodated by diffusive reacceleration, which shifts the spectrum to higher energies.³² Alternatively, one can have a strong increase of the diffusion coefficient at low energies because of the damping of the Alfvén waves,³³ thus reducing the B/C ratio at low energies as well.

Both stable and unstable nuclei are produced in supernovae (SNe) explosions with a ratio given by their known production cross sections. From the decay time and the remaining amount of the unstable nuclei one can reconstruct the time of CRs needed for their journey from the source to our local cavity, so they act as “cosmic clocks”. Such measurements yield an average residence time of CRs in the Galaxy of the order of 10^7 yrs. Since they travel with relativistic speeds the long residence time requires that they cannot move rectilinear from the source to us or to outer space, but the CRs must be scattering many times without losing too much energy, i.e. the diffusion must be effective. During their journey CRs may interact with the gas in the Galaxy and produce secondary particles. This changes the ratio of secondary/primary particles, like the B/C ratio. From the residence time and the amount of secondaries one can estimate the grammage, i.e.

the amount of matter traversed by a CR during its lifetime t_{CR} , which is given by ρct_{CR} , where ct_{CR} is the path length for a particle traveling with the speed of light c . It was found to be of the order of $10\text{g}/\text{cm}^2$, which corresponds to a density of about $0.2\text{ atoms}/\text{cm}^3$.^{34,35} This is significant lower than the averaged density of the disk of $1\text{ atom}/\text{cm}^3$, which suggests that CRs travel a significant time in low density regions, like the halo.

The most advanced program providing a numerical solution to the diffusion equation is the publicly available GALPROP code.³⁶⁻³⁸ The basic parameters are the injection spectrum parameters, the diffusion coefficient, the convection speed, the Alfvén speed and the size of the halo. The latter determines the CR residence time inside the Galaxy, since as soon as they pass the border, they are assumed to escape to outer space. By tuning these parameters to the secondary/primary spectra and the unstable/stable spectra one obtains a self-consistent propagation model of our Galaxy. The amount of secondary CR particles and gamma rays are described by this model by the cross sections of the interactions of the primary and secondary CR with the gas of the disk using a network with more than 2000 cross sections. This is one of the great triumphs of GALPROP.

Remaining problems are connected with the large scale structure of the propagation in the Galaxy, as sampled by gamma rays. The problems are twofold. First of all the gamma rays in the GeV range, which are mainly produced by inelastic collisions of CRs with the gas of the disk, show a too small radial gradient: large amounts of gamma rays are produced at large longitudes, i.e. towards the Galactic anticentre. This is unexpected, since the main sources of CRs are assumed to be the SNe explosions, which are preferentially located at radii of a few kpc. In addition the gas decreases at large radii and the gamma ray flux is proportional to the cosmic ray density times the gas density. This problem can be remedied by assuming much more gas at large radii than determined from the molecular hydrogen (H_2) tracer, which is the $\lambda = 2.6\text{ mm}$ line for the $J=1$ to $J=0$ transition of the carbon monoxide (CO) molecule. This is a good tracer since CO gets excited by collisions with H_2 molecules. Explaining additional gas at large radii requires a strong radial dependence of the ratio $X_{CO} = N(H_2)/N(CO)$, i.e. X_{CO} increases by an order of magnitude from the inner Galaxy to the outer Galaxy.³⁹ An alternative explanation is provided by the Galactic wind models, in which case the transport from the disk to the halo is provided by the mass outflow from the disk to the halo from the SNe explosions, which has a strong radial dependence because of the strong radial dependence of the observed SNR.⁴⁰ This leads to strong anisotropic propagation with the convection being strongest in the regions with the highest cosmic ray pressure from the SNR, i.e. at distances between 4 and 10 kpc. At smaller radii the gravitational potential of the bulge limits the outflow, while at

larger radii the CR pressure decreases.⁴⁰ This reduces the CR intensity in the disk and the corresponding gamma ray production at the position of the sources.

The second GALPROP problem is its failure to describe the EGRET excess of gamma rays, which can be remedied by dark matter annihilation, as discussed in section 2. If one attributes the EGRET excess to DMA one runs into the problem of a too large flux of antiprotons, as discussed in detail by Bergström et al.¹⁰ We have implemented the DMA as a source term into the publicly available GALPROP code^b and find a similar result, as shown in the left panel of Fig. 4 This is not surprising, since GALPROP uses the same priors as the program used by Bergström et al.¹⁰ (i) the propagation is dominated by diffuse scattering, which is assumed to be isotropic, i.e. the same in the halo and the disk (ii) the gas in the disk is smoothly distributed (iii) the influence of observed regular magnetic fields can be neglected. These priors fulfill the basic picture of the origin and propagation of cosmic rays discussed above. The main reason for the large flux of antiprotons from DMA is *not* that DMA produces so many antiprotons, but the fact that the residence time of charged particles is required to be of the order of 10^7 yrs, as determined from the cosmic clocks. The last requirement can be fulfilled in a model with isotropic diffusion only with a large halo, so CRs do not escape, but they perform random walks in a large volume. In this case there is no difference between primary particles produced by SNe or primary particles produced by DMA, so *all* CRs are stored inside the Galaxy. In this case DMA increases the averaged density of antiprotons by orders of magnitude, so the flux of antiprotons becomes of the same order of magnitude as the EGRET excess. Note that the production ratio of antiprotons/gammas from DMA is only at the percent level, as is well known from accelerator experiments for the fragmentation of mono-energetic quarks. If one assumes that the propagation is *not* isotropic, the picture completely changes: the DMA antiprotons may be transported quickly to the halo by a combination of convection or fast diffusion along the regular magnetic fields depicted in Fig. 5. Such an anisotropic propagation model will be discussed in the next section.

4. The Antiproton Flux from DMA in an Anisotropic Propagation Model

The propagation picture with isotropic propagation, as discussed above, is based on hydromagnetic wave theories, in which the turbulent small-scale components of the magnetic field dominate over or are at the same order of magnitude as the regular large scale components. However, the turbulence is expected to be different in the halo and the disk, since the disk is not fully ionized in contrast to the

^bThe GALPROP code can be obtained from <http://galprop.stanford.edu/>.

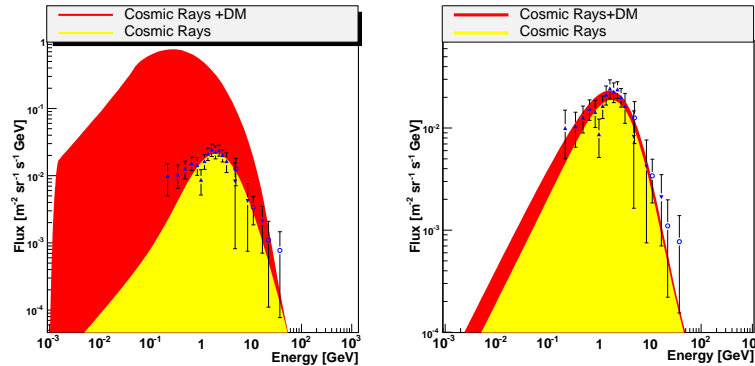


Fig. 4: Comparison of the antiproton production including DMA in the conventional model with isotropic propagation (left) and a model with anisotropic propagation (right).

halo. This implies that the Alfvén waves are efficiently dissipated in the disk by ion-neutral damping. Furthermore the most important contribution to the random field in the disk is by turbulent mass motions, induced by supernova explosions and other stellar mass loss activity, which leads to a different wave spectrum in the disk as compared to the halo, thus leading to different diffusion coefficients in the halo and disk.⁴⁰ In addition one expects the diffusion along the regular magnetic fields to be an order of magnitude faster than the diffusion perpendicular to the magnetic fields, even if the turbulent component is of the same order of magnitude (see e.g.⁴⁰ and references therein). These analytical estimates of fast diffusion along the regular magnetic field lines as compared to the transverse diffusion were confirmed by following the trajectories of CRs in realistic magnetic fields with both a regular and turbulent component. Given the toroidal field in the disk^{41,42} found that the diffusion along the azimuthal magnetic field is one to two orders of magnitude faster than the transverse diffusion. This means that CRs preferentially diffuse along the toroidal fields just above or below the disk or into the halo via the poloidal fields sketched in Fig. 5.^{43–45} In such a picture our local cavity is situated between two thick pancake-like structures of higher CR density only 300 pc apart in the z -coordinate. This leads to a reduced grammage compared with the CR density, which is maximal in the disk, a longer residence time, a reduced radial gradient in the gamma ray flux and an isotropization of the CR flux, all features difficult to explain simultaneously in an isotropic propagation models with a source distribution located towards the centre.

Another possible effect concerning charged particles diffusing fast along reg-

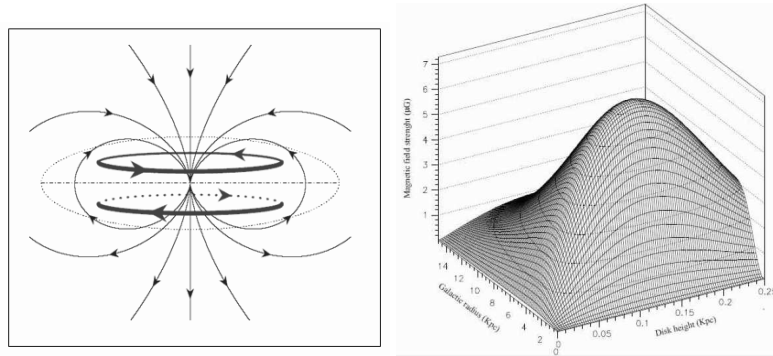


Fig. 5: Left: a schematic picture of the magnetic fields in the Milky Way, consisting of a dipole (poloidal) field component (strongest in the center) and a circular (toroidal) field component, which is strongest just above and below the disk at a distance of 150 pc (from Ref.⁴⁵). Right: a parametrization of the toroidal component (from Ref.⁴²).

ular magnetic field components is related to the molecular clouds: the gas density in the disk varies from 10^{-3} cm^{-3} in the warm ionized medium to $10^2\text{-}10^3 \text{ cm}^{-3}$ in clumps of cold gas with a size of a few pc. In the centre of these clumps the density may be as high as 10^7 cm^{-3} in dense molecular clouds (MC), where star formation occurs. On average the gas density is 1 cm^{-3} in the disk. Inside these MC magnetic fields far above the random components have been observed (see Ref.⁴⁶ for an excellent review). What is more important, these fields seem to be correlated with the observed static magnetic fields outside the MCs.⁴⁷ This can only be understood, if the MCs remember the large scale magnetic fields in the interstellar medium, i.e. if during the contraction flux freezing occurs. In this case the magnetic field lines from the ISM will become highly concentrated near the MCs and CRs in the ISM, which preferentially diffuse fast along these field lines, will be reflected by the higher density of the field lines near the MCs. So, as worked out by Chandran,⁴⁸ the MC act like magnetic mirrors for CRs, just like the concentration of magnetic field lines near the poles from the earth trap the CRs in the famous Van Allen radiation belts. The large distances (10-100 pc scale) between the MC allows to trap particles up to the TeV scale, thus increasing the grammage and the residence time, which are now increased by the trapping time between the MC in the disk, *not* by how often they pass from the halo to the disk, as is the case in the isotropic propagation model. So the halo size is not a sensitive parameter anymore and particles, once in the halo, will be preferentially transported away from the disk by a combination of convection or fast diffusion along the regular field

lines in the halo. It should be noted that only a small fraction of the CRs enter the MCs, if these act as magnetic mirrors. This could explain why positrons mainly annihilate in the gas *between* the MCs, not with electrons from molecular hydrogen *inside* the MCs, as deduced from the annihilation line shape.^{49,50} Of course, one could argue that although the MCs make up the largest mass fraction, they have the lowest filling factor. But if they have strong magnetic fields, the CRs are expected to be tunneled towards the MCs by the high concentration of magnetic field lines.

How can one implement such a propagation model? Existing programs are not suitable. E.g. the CR tracing programs calculating the trajectories in a magnetic field do not calculate all secondary particles and the GALPROP program with isotropic diffusion does not have a regular magnetic field in the propagation of charged particles. However, the basic modifications needed are: the propagation follows preferentially the regular magnetic field lines, which are toroidal in the disk and poloidal in the halo. Such a propagation would require tuning the 3D version of GALPROP. However, this takes an excessive amount of CPU time. Therefore transporting the CRs to the halo by a combination of fast diffusion and convection in the z-direction in the 2D version is much more effective and leads to the same effect: CRs in the halo will hardly come back to the disk. But it should be kept in mind that the parameters are effective parameters in a simplified axisymmetric 2D version of the 3D reality, which has also preferred diffusion directions in the disk.

We have modified the publicly available source code of GALPROP by (i) allowing for a diffusion tensor instead of a diffusion constant, thus modifying the diffusion equation and the Crank-Nickelson coefficients accordingly; (ii) allowing an inhomogeneous grid in order to have step sizes below 100 pc in the disk region and large step sizes in the halo; (iii) implement the dark matter annihilation as a source term of stable primary particles, especially antiprotons, positrons and gamma rays. The dark matter distribution was taken to be the one obtained from the EGRET excess, as discussed above. The grammage and escape time were adjusted for charged particles to account for the fact that secondary particles are now produced largely locally, since particles produced far away from the solar system are likely not to reach our local cavity. If in addition the trapping between molecular clouds is effective, only a small fraction of CRs will penetrate the MCs and most of them will be reflected. But the grammage in between the MCs will be enhanced by the multiple passages from the mirroring, so one would expect it to increase the grammage and residence time by the same factor. This turns out to be working, so this was simply introduced in GALPROP as a constant g , called grammage parameter, multiplying the HI and HII gas densities. A grammage parameter

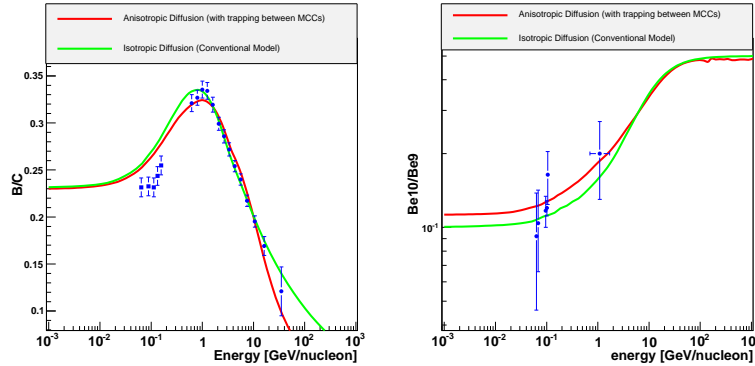


Fig. 6: Comparison of the secondary/primary (B/C) ratio and unstable/stable ($^{10}\text{Be}/^9\text{Be}$) ratio in the conventional model with isotropic propagation and model with anisotropic propagation.

of about 12 is needed to describe the B/C ratio combined with the $^{10}\text{Be}/^9\text{Be}$ ratio. Note that this grammage parameter determines the local production of charged particle, so this grammage parameter is not necessarily the same as the grammage needed for the gamma ray production, since the latter is determined by the large scale gas densities. Given the large fluctuations in and strong radial dependence of the gas densities the difference can be large. Also the CR density is expected to have a radial dependence because of the convection having a radial dependence, as discussed before. The CR density can also have strong variations from the fact that Alfvén waves can be damped in high density gas regions, thus leading to strong variations in the diffusion coefficient and corresponding CR density variations.

The transport from the disk to the halo is quite uncertain. It should be noted that the average scale height of SNIa is expected to be about 300 pc (thick disk) and the ejecta connect to the halo in chimney like structures (see e.g. Ref.^{51,52} and references therein), which can drive magnetic field lines towards high altitudes (≈ 1 kpc), thus facilitating the transport to the halo by the fast parallel diffusion. This was simulated as an enhanced convection term starting at $v_0 = 250\text{km/s}$ at 100 pc above the disk and then increasing with the distance z above the disk as $dv/dz = 37\text{km/s}$. The remaining GALPROP parameters can be found in Ref.⁵³ As shown in Figs. 4 and 6 the antiproton flux, the B/C ratio and the $^{10}\text{Be}/^9\text{Be}$ ratio are all well described by this set of parameters. Clearly, the excess of diffuse gamma rays can be well described together with the B/C ratio and the antiprotons.

In summary, we do not believe that the DMA interpretation of the EGRET is "excluded by a large margin" because of the overproduction of antiprotons as

claimed by Bergström et al.¹⁰ Such a statement is only valid *within their propagation model based on isotropic propagation*. Anisotropic models with different propagation in the halo and the disk can perfectly describe all observations including DMA.

5. Positron Annihilation in our Galaxy

Additional support for the propagation picture with anisotropic propagation, as discussed in section 4, comes from the positron annihilation signal observed by the INTEGRAL satellite.^{11,12} Since positron annihilation is only efficient at non-relativistic energies, the positrons must have energies in the MeV range. Sources of such positrons are largely coming from the decay of radioactive nuclei expelled by dying stars, especially SNIa, since in this case the core makes up a large fraction of the mass. This makes it easier for the positrons to escape from the relatively thin layer of the ejecta. Light curves, which are sustained first by the gamma rays in the shock waves and later by the electrons and positrons, suggest that only a few percent of the positrons escape from the ejecta and can annihilate outside after thermalization. Positrons annihilating inside the ejecta will produce also gamma rays, but these will not be visible as a single 511 keV line because of further interactions in the shock wave.

The main observation is that the 511 keV line from the annihilation between thermalized positrons and electrons (either free or bound in nuclei) is largely confined to the bulge with a bulge/disk (B/D) ratio of a few,^{11,12} although additional data suggests a lower ratio.⁵⁴ Taking the dominant source to be SNIa, one would expect a B/D ratio to be well below one, because of the higher mass in the disk and the higher rate of SNIa explosions expected in the thick disk as compared to the bulge.⁵⁵ An additional problem presents the observation of the 1.8 MeV line from the ²⁶Al radioactive isotope, which has clearly been observed, both in the bulge *and* the disk by the Comptel detector on NASA's CGRO observatory.⁵⁶ These nuclei are thought to be produced by nucleosynthesis in massive stars in the thin disk and yield in their decay on average 0.85 positrons. Because of their non-relativistic speed and high charge ²⁶Al nuclei lose their kinetic energy rapidly and decay with a half life time of about 10⁶ years close to the position where they were created. The observed flux of positron annihilation in the disk seems to be saturated already by the positrons from ²⁶Al and ⁴⁴Ti decays.¹¹ So what happened to the positrons from SNIa explosions in the disk?

In an anisotropic propagation model a large B/D ratio for the positrons is expected, since the bulge is a much more extended object than the disk, so the particles have much more time to thermalize and annihilate in the bulge than in the disk before reaching the halo. Once in the halo they move away from the disk, where

there is hardly any gas for them to annihilate. As mentioned before the fountain like structures of SNR (see e.g. Refs.^{51,52} and references therein) can drive magnetic field lines towards high altitudes (≈ 1 kpc), thus facilitating the transport to the halo by the fast parallel diffusion for the relativistic positrons.

A fraction of the positrons escaping the disk may move by the poloidal field to the bulge, thus enhancing the B/D ratio.⁵⁵ So the problem of the large B/D ratio for positron annihilation is intimately related to the propagation of the positrons. In a conventional propagation model without magnetic fields and homogeneous gas distributions the positrons annihilate near their source^{49,50} and one must resort to new positron sources specific for the bulge, like DMA of very light WIMPS.^{13,57} The WIMP masses have to be below of few MeV, since else they would be visible by synchrotron radiation above the limits set by Comptel and EGRET.^{58,59} In anisotropic propagation models the low strength of the annihilation signal in the disk is simply a consequence of the fact that the disk is so thin, so positrons can escape easily to the halo, where they find no partners to annihilate. So it is the same solution required by the ratio of antiprotons and EGRET excess of gamma rays: fast diffusion perpendicular to the disk either by the regular magnetic fields or convection. In this case no unnatural light WIMPs are needed. Such light WIMPs would need additionally new gauge bosons to have a large enough annihilation cross section compatible with Eq. 1.

6. Constraints from direct dark matter search experiments

Direct detection experiments search for signals of dark matter particles elastically scattering off the nuclei in their detector. The event rate is given by $\Gamma = \langle \sigma v \rangle n$, where n is the local number density of WIMPS, v the velocity between detector and WIMP and σ the scattering cross section. The brackets indicate that the average over the velocity distribution and corresponding cross sections has to be taken. No positive results have been reported and experimental limits on the cross section have been derived under the assumption that the local density of WIMPS corresponds to $0.3 \text{ GeV}/\text{cm}^3$, as estimated from the rotation curve (see e.g. a recent review by Spooner⁶⁰). The best limit obtained by the XENON10 experiment is about $5 \cdot 10^{-8}$ pb at 90% C.L. for a 50 GeV WIMP.⁶¹ This is below the cross section limit expected from the EGRET data, if one assumes the minimal supersymmetric model to be valid. The region allowed by all constraints (WMAP, LEP limits on charginos and Higgses, $b \rightarrow s\gamma$ branching ratio, EGRET mass limits) is shown in Fig. 7 together with the limits from some typical direct dark matter search experiments.⁶² No signal was found so far, so the regions above these lines are excluded. Naively one could conclude that the DMA interpretation of the EGRET excess combined with all electroweak and relic density constraints

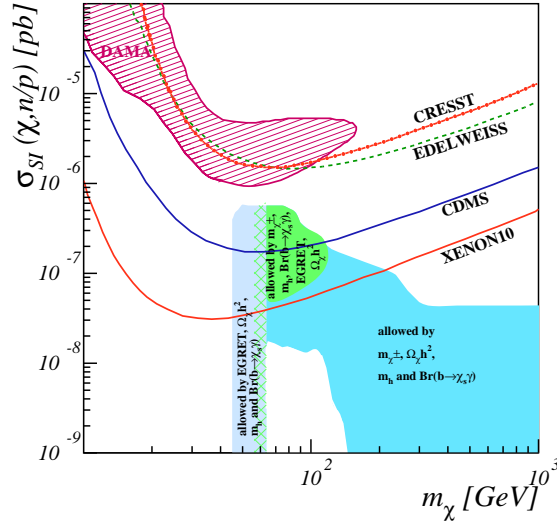


Fig. 7: The spin-independent cross section for neutralino-nucleon scattering compared with experimental constraints: the region above the XENON10 limit is excluded. Details can be found in Ref.⁶²

(green region in Fig. 7) is excluded by the XENON10 data. However, there are severe caveats. First of all, the event rate in these experiments is proportional to the cross section *and* the local WIMP density. Both have large uncertainties: the cross section is model dependent and has only been calculated in the minimal supersymmetric models. Although the EGRET data is perfectly consistent with supersymmetry, it does not prove supersymmetry and in e.g. extra dimension models the cross sections could be very different. Secondly the local relic density has large uncertainties, because the densities obtained from the rotation curve do not say anything about the clustering of dark matter, but yield only an averaged density. From N-body simulations one knows that dark matter is clumpy, as can be expected already from the fact that galaxies are formed by dark matter starting to pull together from the initial density fluctuations in the early universe. The number of clumps is very large because of the steep decrease of the mass spectrum with increasing mass ($\propto M^{-2}$) and the lightest clumps are very light (about $10^{-6}M_\odot$, see Ref.⁶³). But even with this large number of clumps the probability of finding a clump in the solar neighbourhood is small, so the direct searches are more likely to observe first interactions from the diffuse component, which originates from the

tidal stripping of the clumps. How many are disrupted is an ongoing debate (see e.g. Refs.^{64,65}), but it certainly depends sensitively on the dark matter profile of the clumps. These profiles cannot be calculated yet reliably from N-body simulations. It is conceivable that the density of the diffuse component is an order of magnitude less than the clumpy component, so any statements concerning exclusions from direct dark matter detection experiments should take this into account.

7. Conclusion

With an anisotropic propagation model the amount of antiprotons expected from DMA annihilation can be reduced by one to two orders of magnitude. Therefore the claim by Bergström et al.¹⁰ that the DMA interpretation of the EGRET excess of diffuse Galactic gamma rays is excluded “by a large margin” is strongly propagation model dependent. It only applies for their simplified propagation model, which assumes the same diffusion in the halo and in the disk. An anisotropic propagation model with different propagation in the halo and the disk can reconcile the EGRET excess with the antiproton flux and the ratios of secondary/primary and unstable/stable nuclei. In addition the difference in geometry between bulge and disk leads to much more radiation and annihilation of positrons and electrons in the bulge as compared to the disk, thus alleviating the need to introduce new sources of positrons and electrons for the bulge to explain the INTEGRAL excess of the 511 keV line in the bulge.¹³ Direct dark matter search experiments reach the cross section range expected from the EGRET excess. However, the experimental limits are inversely proportional to these cross sections times the local relic density. Both are uncertain: for the cross section one assumes the WIMPS are the lightest supersymmetric partners of the minimal supersymmetric model with gravity inspired breaking of supersymmetry, while for the local relic density one assumes the WIMPS are smoothly distributed instead of the expected distribution in clumps. The clumpy nature can drastically reduce the local density if we are not located inside a clump.

In summary we consider DMA is a viable explanation of the EGRET excess of diffuse Galactic gamma rays, especially since it is observed with the same shape of the fragmentation of mono-energetic quarks in all sky directions and the intensity distribution of the excess traces the DM profile, as shown independently by the rotation curve, the gas flaring and the N-body simulation of the disruption of the Canis-Major satellite galaxy.

8. Acknowledgements

I wish to thank the organizers for the kind invitation to this splendid conference. Furthermore I thank P. Blasi, D. Breitschwerdt and N. Prantzos for helpful discussions and my close collaborators I. Gebauer, D. Kazakov, M. Weber and V. Zhukov for their contributions.

This work was supported by the BMBF (Bundesministerium für Bildung und Forschung) via the DLR (Deutsches Zentrum für Luft- und Raumfahrt).

References

1. D.N. Spergel et al., *ApJS*, **170** (2007)377.
2. G. Jungman, M. Kamionkowski, and K. Griest, *Phys. Rep.*, **267**(1996)195.
3. E. Kolb, and M.S. Turner, M.S. 1990, *The Early Universe* (Addison Wesley)
4. W. de Boer, C. Sander, V. Zhukov, A.V. Gladyshev and D.I. Kazakov, *Phys. Lett. B* **636** (2006) 13, arXiv:hep-ph/0511154.
5. L. Bergström, L., *Rep. Prog. Phys.*, **63** (2000) 793; arXiv:hep-ph/0002126.
6. G. Bertone, D. Hooper, and J. Silk, *Phys. Rept.* **405**(2005) 279; arXiv:hep-ph/0404175.
7. T.J. Sumner, 2002, www.livingreviews.org/Articles/Volume5/2002-4sumner; *Living Reviews in Relativity* published by the Max Planck Institute for Gravitational Physics, Albert Einstein Institute, Germany.
8. S.D. Hunter, et al., *ApJ*, **481**(1997) 205.
9. W. de Boer, C. Sander, V. Zhukov, A.V. Gladyshev, and D.I. Kazakov, *A&A* 444 (2005) 51 , arXiv:astro-ph/0508617.
10. L. Bergström, L. et al., *JCAP* **0605** (2006) 006, arXiv:astro-ph/0602632.
11. J. Knödseder, *et al.*, *Astron. Astrophys.* **441**(2005) 513, arXiv:astro-ph/0506026.
12. G. Weidenspointner *et al.*, *A&A*, **450** (2006)1013, arXiv:astro-ph/0601673.
13. C. Boehm, D. Hooper, J. Silk, M. Casse and J. Paul, *Phys. Rev. Lett.* **92** (2004) 101301, arXiv:astro-ph/0309686.
14. W.M. Yao, *et al.* [Particle Data Group], *J. Phys. G* **33**2006 1.
15. N.F. Martin, R.A. Ibata, M. Bellazzini, M.J. Irwin, G.F. Lewis and W. Dehnen, *Mon. Not. Roy. Astron. Soc.* **348**(2004) 12, arXiv:astro-ph/0311010.
16. J. Penarrubia et al., *Astrophys. J.* **626** (2005) 128, arXiv:astro-ph/0410448.
17. D. Martinez-Delgado, D.J. Butler, H.W. Rix, Y.I. Franco and J. Penarrubia, *Astrophys. J.* **633** (2005)205, arXiv:astro-ph/0410611.
18. M. Bellazzini, R. Ibata, N. Martin, G.F. Lewis, B. Conn and M.J. Irwin, *Mon. Not. Roy. Astron. Soc.* **366**(2006) 865, arXiv:astro-ph/0504494.
19. Penarrubia, J., Martinez-Delgado, D. and Rix, H.W. 2007, arXiv:astro-ph/0703601.
20. H.J. Newberg et al. *ApJ* **569** (2002) 245.
21. B. Yanny et al. *ApJ*, **588** (2003) 824 [Erratum-ibid. **605** (2003) 575]; arXiv:astro-ph/0301029.
22. R.A. Ibata, M.J. Irwin, G.G. Lewis, A.M.N. Ferguson and N. Tanvir, *MNRAS*, **340** (2003) L21; arXiv:astro-ph/0301067. [arXiv:0705.3655 [astro-ph]].
23. H.J. Rocha-Pinto, S.R. Majewski, M.F. Skrutskie, and J.D. Crane, *ApJ* **594** (2003) L115 and arXiv:astro-ph/0307258.

24. M. Lopez-Corredoira, Y. Momany, S. Zaggia and A. Cabrera-Lavers, arXiv:0707.4440 [astro-ph].
25. B.C. Conn et al., Mon. Not. Roy. Astron. Soc. **376** (2007) 939, arXiv:astro-ph/0701664.
26. P.M.W. Kalberla, L. Dedes, J. Kerp and U. Haud, A&A, **469** (2007) 511, arXiv:0704.3925 [astro-ph].
27. A.W. Strong, I.V. Moskalenko and O. Reimer, ApJ, **613** (2004) 962; arXiv:astro-ph/0406254.
28. F.W. Stecker, S.D. Hunter and D.A. Kniffen, arXiv:0705.4311 [astro-ph].
29. D.J. Thompson et al., IEEE Trans. Nucl. Sci., **34** (1987) 36.
30. J.A. Esposito et al., ApJ **123** (1999) 203.
31. R. Kulsrud and W.P. Pearce, ApJ **156** (1969) 445.
32. A. W. Strong, I. V. Moskalenko and V. S. Ptuskin, Ann. Rev. Nucl. Part. Sci. **57** (2007) 285, arXiv:astro-ph/0701517.
33. V.S. Ptuskin, I.V. Moskalenko, F.C. Jones, A.W. Strong and V.N. Zirakashvili, Astrophys. J. **642**(2006) 902, arXiv:astro-ph/0510335.
34. R. Schlickeiser, R., 2002, "Cosmic ray astrophysics," Springer Verlag, Berlin.
35. V.S. Berezhinsky, S.V. Bulanov, V.A. Dogiel, V.L. Ginzburg and V.S. Ptuskin, 1990, "Astrophysics of Cosmic Rays" Amsterdam, North-Holland Publishing.
36. A.W. Strong and I.V. Moskalenko, ApJ, **509** (1998) 212; arXiv:astro-ph/9807150.
37. I.V. Moskalenko, A.W. Strong and O. Reimer, A&A, **338** (1998) L75; arXiv:astro-ph/9808084
38. A.W. Strong, I.V. Moskalenko and O. Reimer, ApJ, **537** (2000) 763 [Erratum-ibid. **541** (2000) 1109]; arXiv:astro-ph/9811296; Details on the latest GALPROP versions can be found at <http://www.mpe.mpg.de/aws/propagate.html>.
39. A.W. Strong, I.V. Moskalenko, O. Reimer, S. Digel and R. Diehl, 2004, A&A **422** (2004) L47, arXiv:astro-ph/0405275.
40. D. Breitschwerdt, V.A. Dogiel and H.J. Völk, A&A, **385** (2002) 216, arXiv:astro-ph/0201345.
41. D. De Marco, P. Blasi and T. Stanev, JCAP **0706** (2007) 027, arXiv:0705.1972 [astro-ph].
42. A. Codino and F. Plouin, arXiv:astro-ph/0701498.
43. J.L. Han, R.N. Manchester, E.M. Berkhuijsen and R. Beck, A&A, **322** (1997) 98
44. J.L. Han, Ap&SS, **278** (2001) 181, arXiv:astro-ph/0010537.
45. J.L. Han, Chin. J. Astron. Astrophys. **6** (2006) 211, astro-ph/0603512v2.
46. C. Heiles and R. Crutcher, in "Cosmic Magnetic Fields", 2005, Eds. Richard Wielebinski and Rainer Beck. Lecture notes in Physics Volume 664, publ. by Springer, Berlin, Germany, p. 137, arXiv:astro-ph/0501550.
47. J.L Han and J.S. Zhang, A&A **464** (2007) 609, arXiv:astro-ph/0611213.
48. B.D.G. Chandran, Space Sci. Rev. **99** (2000) 271, arXiv:astro-ph/0010105.
49. P. Jean, et al., Astron. Astrophys. **445** (2005) 579, arXiv:astro-ph/0509298.
50. N. Guessoum, P. Jean and W. Gillard, A&A **436** (2005) 171, arXiv:astro-ph/0504186.
51. M.A. de Avezil and D. Breitschwerdt, Astron. Astrophys. **425** (2005) 899, [arXiv:astro-ph/0407034].
52. M.A. de Avezil and D. Breitschwerdt, Proc. of the XXXIXth Rencontres de Moriond, La Thuile, Aosta Valley, Italy, March 21 - 28, 2004, Eds. T. Montmerle,

- A. Chalabaev, J. Tran Thanh Van, arXiv:astro-ph/0502078.
53. I. Gebauer, arXiv:0710.4966 [astro-ph].
 54. G. Weidenspointner *et al.* 2007, arXiv:astro-ph/0702621.
 55. N. Prantzos, A&A **449**(2005) 869, arXiv:astro-ph/0511190.
 56. Diehl, R. *et al.*, Nature **439** (2006) 45, [arXiv:astro-ph/0601015].
 57. Y. Ascasibar, P. Jean, C. Boehm and J. Knödseder, Mon. Not. Roy. Astron. Soc. **368**(2005) 1695, arXiv:astro-ph/0507142.
 58. J.F. Beacom, N.F. Bell, and G. Bertone, Phys. Rev. Lett. **94**(2005) 171301, arXiv:astro-ph/0409403.
 59. C. Boehm and P. Uwer, arXiv:hep-ph/0606058.
 60. N. J. Spooner, arXiv:0705.3345 [astro-ph].
 61. J. Angle *et al.* [XENON Collaboration], arXiv:0706.0039 [astro-ph].
 62. J. Deger-Glaeser, “Kombination von direkter und indirekter Such nach dunkler Materie, Diplomarbeit, Univ. of Karlsruhe, 2007.
 63. J. Diemand, B. Moore and J. Stadel, Nature **433**(2005) 389 arXiv:astro-ph/0501589.
 64. B. Moore, J. Diemand, J. Stadel and T. Quinn, arXiv:astro-ph/0502213.
 65. V. Berezhinsky, V. Dokuchaev and Y. Eroshenko, Phys. Rev. D **73**, 063504 (2006), arXiv:astro-ph/0511494.